

RESEARCH

Open Access



# Gingival shape analysis using surface curvature estimation of the intraoral scans

Marko Kuralt<sup>1,2\*</sup> , Alja Cmok Kučič<sup>3</sup>, Rok Gašperšič<sup>4,5</sup>, Jan Grošelj<sup>6</sup>, Marjeta Knez<sup>6</sup> and Aleš Fidler<sup>1,7</sup>

## Abstract

**Background:** Despite many advances in dentistry, no objective and quantitative method is available to evaluate gingival shape. The surface curvature of the optical scans represents an unexploited possibility. The present study aimed to test surface curvature estimation of intraoral scans for objective evaluation of gingival shape.

**Methods:** The method consists of four main steps, i.e., optical scanning, surface curvature estimation, region of interest (ROI) definition, and gingival shape analysis. Six different curvature measures and three different diameters were tested for surface curvature estimation on central (n = 78) and interdental ROI (n = 88) of patients with advanced periodontitis to quantify gingiva with a novel gingival shape parameter (GS). The reproducibility was evaluated by repeating the method on two consecutive intraoral scans obtained with a scan-rescan process of the same patient at the same time point (n = 8).

**Results:** Minimum and mean curvature measures computed at 2 mm diameter seem optimal GS to quantify shape at central and interdental ROI, respectively. The mean (and standard deviation) of the GS was  $0.33 \pm 0.07$  and  $0.19 \pm 0.09$  for central ROI using minimum, and interdental ROI using mean curvature measure, respectively, computed at a diameter of 2 mm. The method's reproducibility evaluated on scan-rescan models for the above-mentioned ROI and curvature measures was 0.02 and 0.01, respectively.

**Conclusions:** Surface curvature estimation of the intraoral optical scans presents a precise and highly reproducible method for the objective gingival shape quantification enabling the detection of subtle changes. A careful selection of parameters for surface curvature estimation and curvature measures is required.

**Keywords:** Gingivitis, Periodontitis, Computer-assisted image analysis, Dental model, Shape analysis, Curvature, Optical scanning

## Background

Detection and diagnosis of gingival and periodontal conditions is a complex process requiring knowledge, experience, and skills [1]. First, gingival tissues are assessed for the presence or absence of inflammation by assessing the tissues' redness and degree of swelling descriptively or as part of various qualitative or semi-quantitative indices [2–4]. Further examination also includes an invasive but

more objective component evaluating the tissues' tendency to bleed upon provocation using the periodontal probe in a dichotomous or semi-quantitative manner [1, 2]. Finally, a gingival morphology [5] and gingival phenotype, i.e., gingival thickness and keratinized tissue width, that can be altered with teeth malposition [6, 7] should be evaluated as a part of periodontal phenotype evaluation also including an evaluation of bone morphotype, i.e., buccal bone thickness. A wide variety of novel imaging methods are constantly being proposed to aid in the diagnosis of periodontal conditions, including ultrasound imaging [8], magnetic resonance imaging [9], cone-beam computed tomography [10, 11], optical coherence

\*Correspondence: marko@kuralt.si

<sup>1</sup> Department of Restorative Dentistry and Endodontics, University Medical Centre Ljubljana, Hrvatski trg 6, 1000 Ljubljana, Slovenia  
Full list of author information is available at the end of the article



© The Author(s) 2022, corrected publication 2022. **Open Access** This article is licensed under a Creative Commons Attribution 4.0 International License, which permits use, sharing, adaptation, distribution and reproduction in any medium or format, as long as you give appropriate credit to the original author(s) and the source, provide a link to the Creative Commons licence, and indicate if changes were made. The images or other third party material in this article are included in the article's Creative Commons licence, unless indicated otherwise in a credit line to the material. If material is not included in the article's Creative Commons licence and your intended use is not permitted by statutory regulation or exceeds the permitted use, you will need to obtain permission directly from the copyright holder. To view a copy of this licence, visit <http://creativecommons.org/licenses/by/4.0/>. The Creative Commons Public Domain Dedication waiver (<http://creativecommons.org/publicdomain/zero/1.0/>) applies to the data made available in this article, unless otherwise stated in a credit line to the data.

tomography [12], and optical scanning [13]. Recently, intraoral scans were utilized for the remote diagnosis of gingival and periodontal conditions by visual assessment [14, 15]. Both studies reported promising results regarding time efficiency and accuracy of the remote diagnosis that could be further increased with future technology improvements such as artificial intelligence [16].

In periodontal research, optical scanning enabled novel and accurate evaluation methods, such as volumetric assessment of soft tissue dynamics [17–19]. Recently, computer-aided analysis of optical scans revealed considerably improved accuracy of linear measurements of dimensional differences of soft tissues after different treatment procedures compared to evaluation with periodontal probe [20–23]. Furthermore, optical scans also present a possibility for shape analysis, successfully implemented in medical image analysis to aid in detecting and diagnosing [24–26]. Recently, palatal morphology was evaluated and compared, enabling twin differentiation or human identification due to the high accuracy of the intraoral optical scanning [27]. A different approach with surface curvature estimation was utilised in a validation study using intraoral optical scans to document palatal soft tissue shape and surface irregularity as a possible screening and diagnostic tool for oral cancer [28]. Furthermore, as visual assessment of gingival inflammation is based on the morphological changes of the gingival tissues [2, 4], it seems that evaluation of such changes by shape analysis might facilitate the detection of subtle changes associated with the presence, progression, and resolution of gingival conditions. Therefore, in both clinical and research settings, there is a need for the non-invasive, objective, and precise evaluation of gingival tissues and their changes.

Therefore, the present study aimed to propose an objective evaluation method for gingival shape analysis using surface curvature estimation of the intraoral optical scans by applying different curvature measures computed at various parameters on central and interdental gingiva.

**Methods**

**Gingival shape analysis**

The proposed method consisted of four main steps, i.e., image acquisition—optical scanning, surface curvature estimation, region of interest (ROI) definition, and gingival shape analysis.

**Acquisition—optical scanning**

The inclusion criterion was the presence of advanced periodontitis (Stage III, Grade B/C; [29]) with at least nine teeth (excluding molars) in the upper jaw. The exclusion criteria were periodontal treatment in the last six months, antibiotic treatment in the previous six

months, chronic systemic diseases, and medication with known influence on periodontium or wound healing. Sixteen maxillary digital models, i.e., two per patient, were acquired in a scan-rescan manner using intraoral optical scanning (CEREC Omnicam AC, Dentsply Sirona; software version: SW 4.5.2). An experienced operator performed two consecutive scans of each patient to obtain the morphology of the tissues without any patient’s or operator’s actions in between the scans. Teeth from right to left premolars were included in the analysis resulting in a dataset of 78 maxillary teeth. One patient was additionally scanned 3-months after the non-surgical treatment of periodontitis to demonstrate the proposed method’s applicability. Digital models were exported in Standard Tessellation Language (STL) file format.

**Surface curvature estimation**

Surface curvature is the quantity that measures how much the surface locally at each point deviates from the plane orthogonal to the surface at that point (called the tangent plane). The amount of deviation depends on the direction we choose in the tangent plane. The two directions where the amount of change is minimum and maximum are called principal curvature directions, and they correspond to the principal curvatures, i.e., maximum curvature  $k_{max}$  and minimum curvature  $k_{min}$  (Fig. 1). These two principal curvatures are eigenvalues of the shape operator [30] and can be combined in several ways to obtain a quantity representing a curvature measure [31], e.g.,

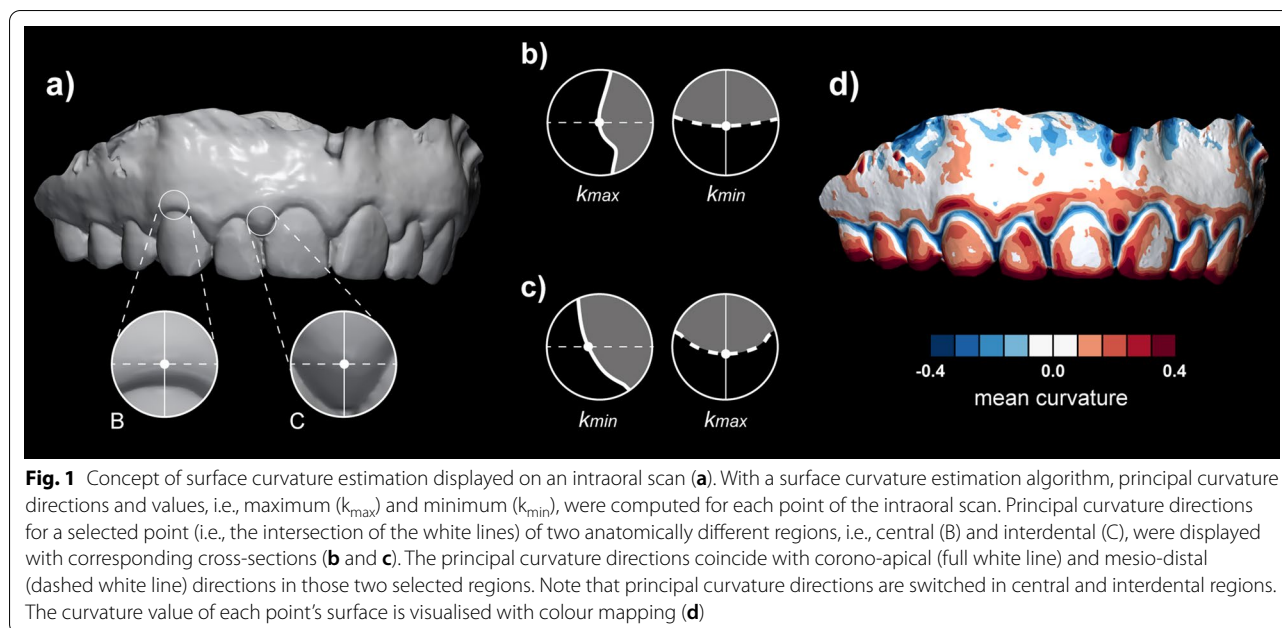
$$mean\ curvature(MC) : H = \frac{k_{max} + k_{min}}{2}$$

$$Gaussian\ curvature(GC): K = k_{max} * k_{min}$$

$$shape\ index(SI) = \frac{2}{\pi} \arctan\left(\frac{k_{min} + k_{max}}{k_{min} - k_{max}}\right) = \frac{2}{\pi} \arctan\left(\frac{-H}{\sqrt{H^2 - K}}\right)$$

$$curvedness(CU) = \sqrt{\frac{k_{max}^2 + k_{min}^2}{2}} = \sqrt{2H^2 - K}$$

Since in our case the scanned surface is not given as a smooth parametric surface, but just as a discrete triangular surface mesh, approximation algorithms must be used to estimate these quantities at each of the vertex of the triangular mesh. From the above formulas it is enough to estimate only the mean (MC) and Gaussian curvature



(GC). The efficient and fast numerical algorithms are local, meaning that only the information of the position of the vertex together with positions of neighbouring vertices (chosen by a prescribed diameter) is used to compute MC and GC at each vertex. These algorithms are usually based on local least square bivariate polynomial or rational approximants [32] or the approximation of the Laplace-Beltrami operator using spatial averages [33].

For our problem the surface curvature was computed using PyMeshLab, i.e., a Python library that interfaces to MeshLab (version 2021.10). A “Scale Dependent Quadric Fitting” curvature estimation method was used, enabling the definition of the diameter of interest. The diameter defines the neighbouring points of each vertex that are used to construct the approximating quadric (rational quadratic) surface, which then allows the computation of curvature measures at the vertex of interest. All curvature measures mentioned above, i.e., MC, GC, SI, CU, and minimum (Min) and maximum curvature (Max) as implemented in the software were computed at three different diameters, i.e., 0.5, 1, and 2 mm (Fig. 2).

Each model was exported in polygon file format (PLY), enabling the model to save computed curvature values for each point as a scalar value.

#### ROI definition

Two ROIs were defined on the gingival margin, i.e., central and interdental (Fig. 3). The ROI was defined with the aid of landmark curves in GOM Inspect (version 2018, GOM GmbH) and 3D Slicer (version 4.11.20210226) [34]. First, the gingival margin was

defined with the method proposed by Kuralt et al. [35] utilizing surface curvature. Then, the gingival margin landmark curve was projected in the apical direction on the model's surface with an offset of 3 mm, thus, limiting the ROI in the apical direction. Next, the tooth's mesial and distal line angles were used to create cross-sections in the coronal-apical direction for mesial and distal limitations, delimiting central from interdental ROI. Finally, defined curves were exported in comma-separated values (CSV) file format.

#### Gingival shape analysis and visualisation

Scans with computed curvature values and landmark curves for ROI definition were imported into the CloudCompare (version 2.12 alpha) for further analysis. All available scans with different curvature values per case were combined into one scan with multiple scalar fields. Thus, enabling standardised ROI selection using the Segment tool. Each ROI's curvature value, i.e., 18 different combinations—six different curvature measures and three diameters, were exported to Excel (Microsoft 365, Microsoft) to calculate descriptive statistics. The distribution of curvature values within the ROI depended on the ROI's size and included geometrical features. The selected ROI also included a small part of the gingival margin (Fig. 3—blue) that shifted the mean values per ROI towards zero (Fig. 3—boxplots and histograms). To avoid this effect, the 95th percentile of the curvature values of each ROI and curvature

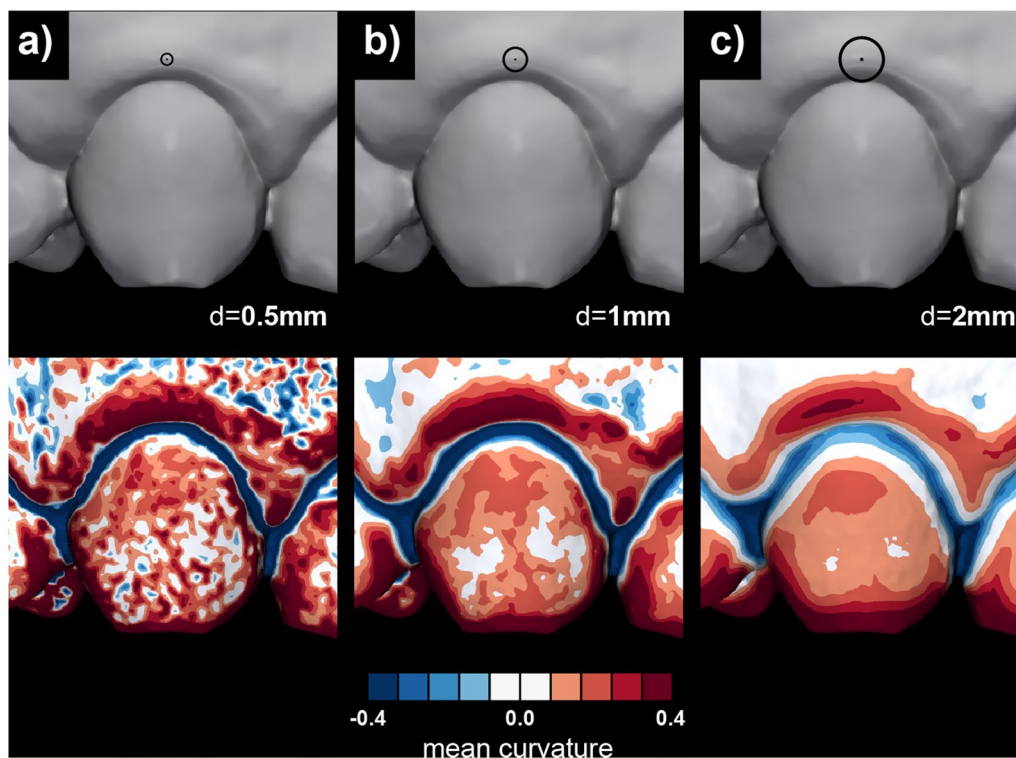


**Fig. 2** The effect of different diameter selection, ranging from 0.5 (a) to 2 mm (c), for surface approximation that gives surface curvature estimation. The diameter represents a threshold for detecting intraoral scans' geometrical features

measure was used to measure the local maximum shape of the gingiva (gingival shape parameter—GS).

Curvature values were visualised only at the gingival margin with a discrete threshold colour scale [36] to facilitate the observation of gingival shape (Fig. 3).

#### Method validation

The reproducibility of surface curvature estimation for gingival shape analysis was evaluated by computing the surface curvature on two consecutive scans acquired at the same time-point with a scan-rescan process. The mean of the absolute differences in the GS, i.e., the 95th percentile of the curvature values in the ROI, was used as a methodological error between scan and rescan at each diameter and curvature measure.

## Results

#### Validation of the proposed method

The curvature values and methodological error of the central and interdental ROI for each curvature measure and diameter are displayed with bar charts similar to signal-to-noise charts.

(Fig. 4). The mean GS of a study sample (Fig. 4—light grey) decreases in all curvature measures with

increasing diameter except for the SI, indicating that all measures except SI are size-dependent (Fig. 4e). Visual inspection of colour-coded curvature maps also confirms a decrease of curvature values with increasing diameter exhibited by the decreased intensity of colours (Fig. 2).

The methodological error, i.e., absolute differences in the GS between scan and rescan values (Fig. 4—dark grey), also decreases with an increasing diameter (Fig. 4). The methodological error represents a minor part in relation to the GS except for the GC and CU measures (Fig. 4b and f).

For central ROI, Min measure computed at 2 mm diameter seems optimal parameter to quantify shape with mean (and standard deviation) of 0.33 (0.07) for a study sample. While MC measure computed at 2 mm diameter seems optimal parameter to quantify shape for interdental ROI with mean (and standard deviation) of 0.19 (0.09) for a study sample.

#### Demonstration of the proposed method

The proposed method for gingival shape analysis using surface curvature estimation was demonstrated in a clinical case of periodontitis treatment (Figs. 5 and 6).

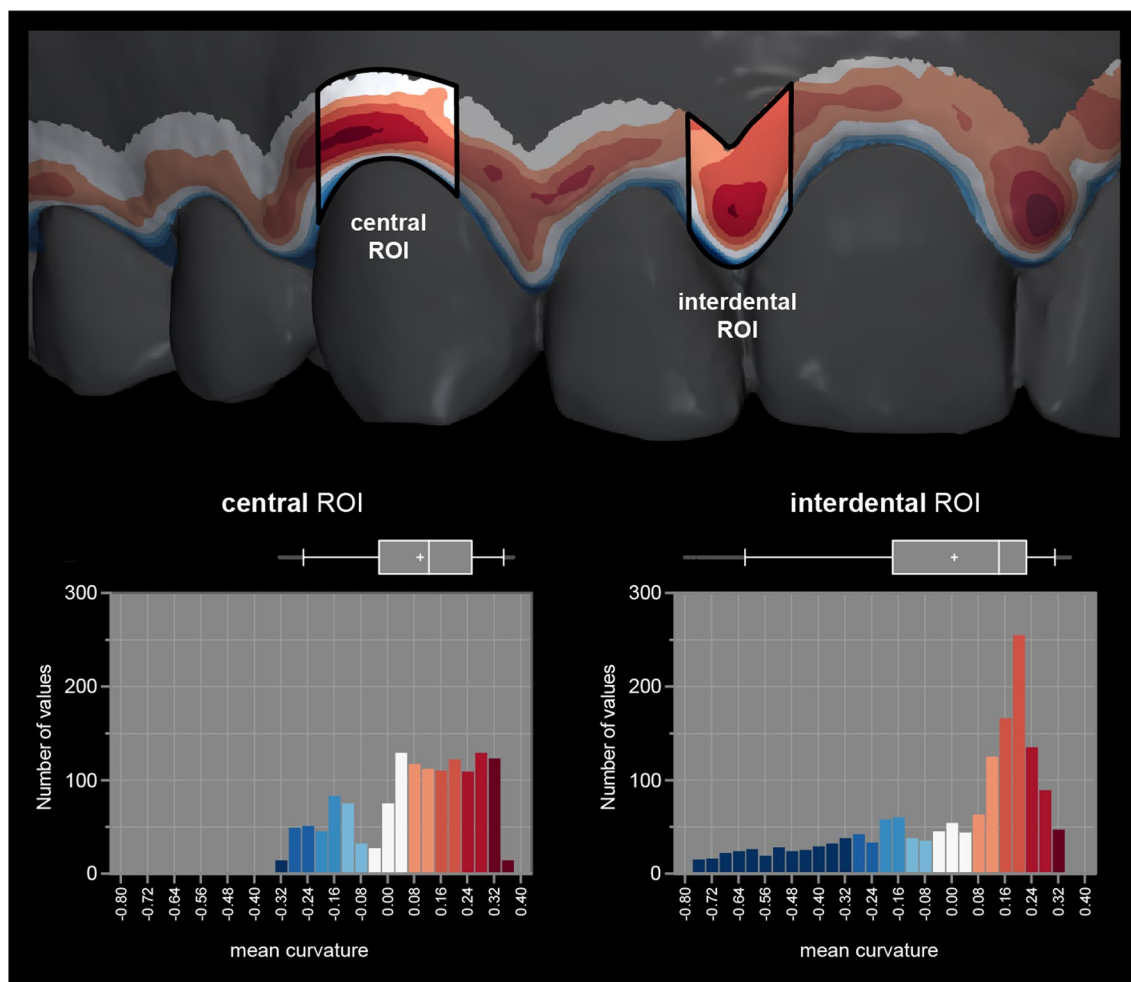


**Fig. 3** Two regions of interest (ROI), i.e., central and interdental, are displayed on a gingival margin band to facilitate focused visualisation. Corresponding histograms and boxplots are shown to display the distribution and variability of the curvature values. Local maximum values (red) are of interest for gingival shape analysis. Whiskers represent 5th and 95th percentile values, and + represents mean value

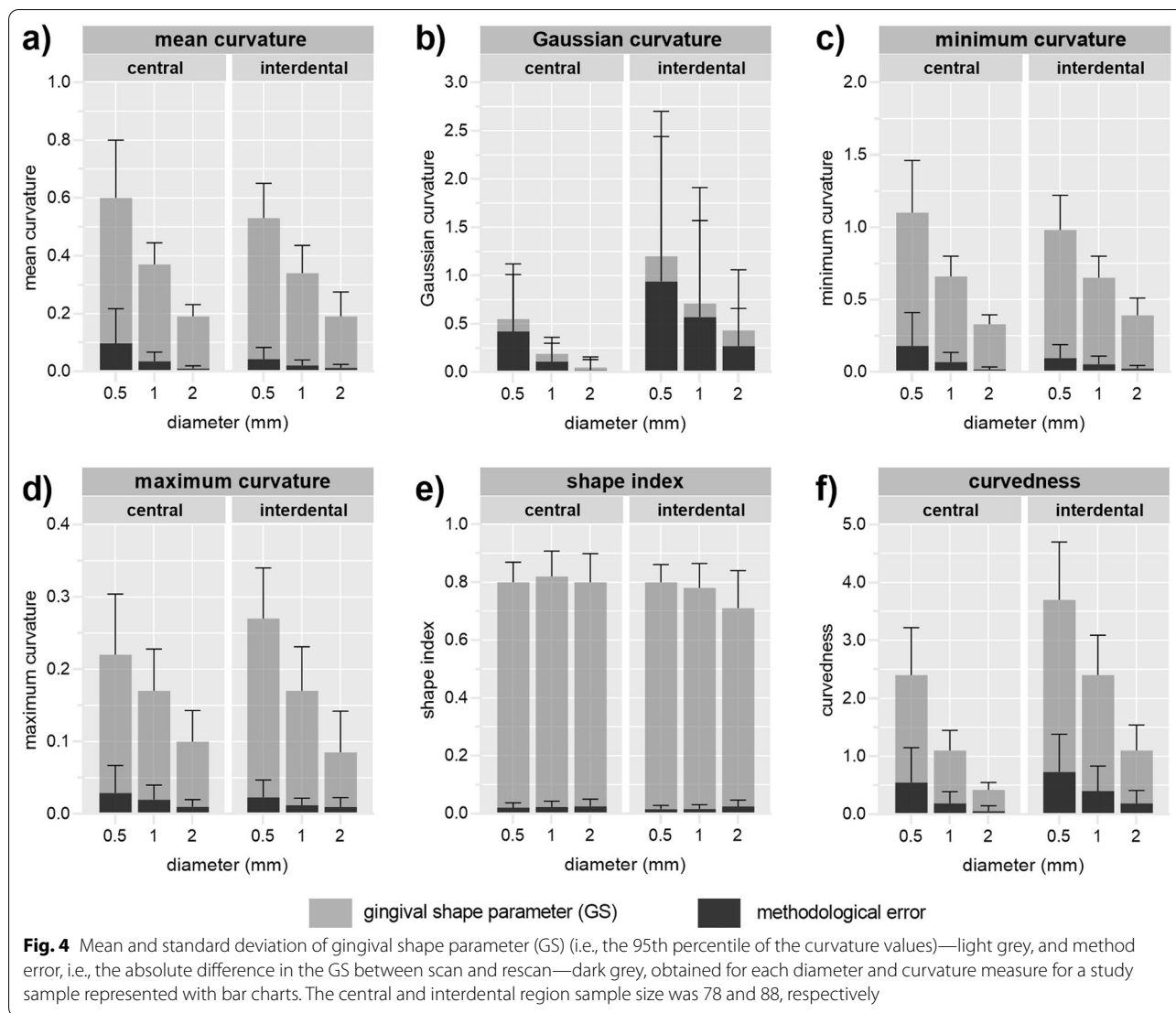
Furthermore, visual observation of the cross-sections displayed in Fig. 1 and colour-coded models with all curvature measures computed at 2 mm diameter (Additional file 1: Fig. 1) confirmed that Min and MC measures seem optimal parameters to quantify shape at central and interdental ROI, respectively.

**Discussion**

The surface curvature estimation of the intraoral scans presents a precise method for gingival shape analysis demonstrated by a high ratio of curvature values versus methodological error. Gingival tissues’ shape seems to be optimally evaluated by the Min for central and MC for interdental region, both computed at 2 mm diameter. Objectively describing and quantifying the gingival tissues’ shape may aid in evaluating morphological variability, detecting and diagnosing early periodontal

conditions, and may play an important role in following changes over time.

To the best of our knowledge, this is the first study attempting to use non-invasive intraoral scans for quantitative evaluation of the gingiva in terms of shape. Many non-invasive digital methods were proposed to overcome the subjectivity of gingival assessment [4]. Those methods are based either on colour changes, i.e., redness [37, 38], or volumetric changes of the tissues, i.e., oedema [13, 39, 40], with the latter indirectly evaluating shape through dimensional differences. In medicine, shape analysis is a well-established approach utilizing various methods [41]. In periodontology, digital evaluation predominantly means just the digitalization of the established evaluation methods [42]. Only recently, curvature analysis was used for segmentation of teeth [43–45] and to detect anatomical landmarks,



i.e., cemento-enamel junction and gingival margin, to automate gingival recession measurements [46] and evaluate changes over time [20, 35]. Surface curvature estimation utilised for the palatal soft tissue shape quantification [28] and the results of the present study indicate that surface curvature estimation of optical scans presents a suitable method for soft tissue shape analysis. The proposed method facilitates detecting subtle changes of the tissues almost not detected by existing methods as observed in colour-coded distance maps (Figs. 5 and 6), proposing complimentary use of the existing and proposed methods. Differences could also be evaluated in baseline gingival shape concerning craniofacial characteristics and periodontal phenotype.

Definition of the diameter for the surface approximation in the surface curvature estimation is essential for optimal detection of gingival shape. Therefore, local

geometric analysis often requires surface modification, i.e., smoothing or surface approximation with a defined diameter of interest prior to the computation [47]. Such surface modification or approximation aims to preserve relevant features and suppress noise and details below a certain threshold of interest for analysis, i.e., the defined diameter. The present study used a local size-dependent curvature estimation method with the diameters defined through empirical observation. The results revealed that robustness to noise increases with an increasing diameter which is also evident with a decrease in methodological error (Figs. 2 and 4). According to the results, a diameter of 2 mm yielded the most relevant colour-coded curvature maps displaying morphologically relevant features (Fig. 2).

Central and interdental gingiva are two distinct regions regarding their shape, affecting the selection of optimal

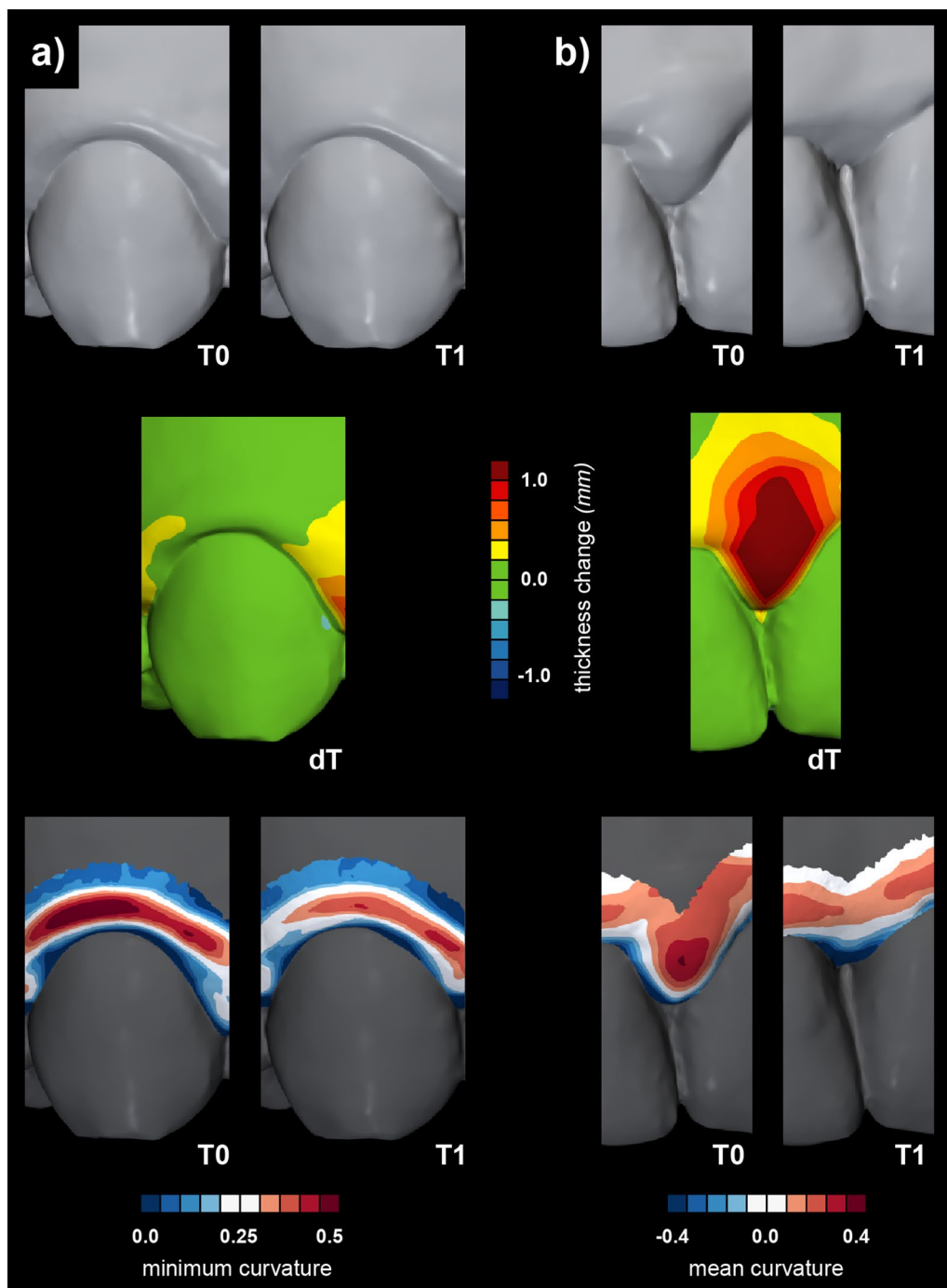


**Fig. 5** The ability of the novel method for gingival shape analysis using surface curvature to detect subtle differences in soft tissue dynamics undetectable by volumetric assessment. Baseline (T0) and three-month follow-up (T1) intraoral scans associated with the non-surgical periodontal treatment (upper row) of two anatomically different regions, i.e., central (a) and interdental (b). The scans were superimposed and evaluated in terms of tissue thickness changes (middle row) and with a novel gingival shape analysis (bottom row). Changes in the interdental regions are already apparent when comparing the scans side by side and even more pronounced with the volumetric colour-coded map. Changes are also confirmed with the gingival shape analysis using mean curvature measure (b). It should be outlined that the region for gingival shape analysis also shifted in the apical direction with the loss of the tissues. However, the regions were defined wide enough to capture the local maximum. In contrast, changes in central regions are subtle and barely visible with direct observation but are demonstrated by gingival shape analysis using minimum curvature measure (a)

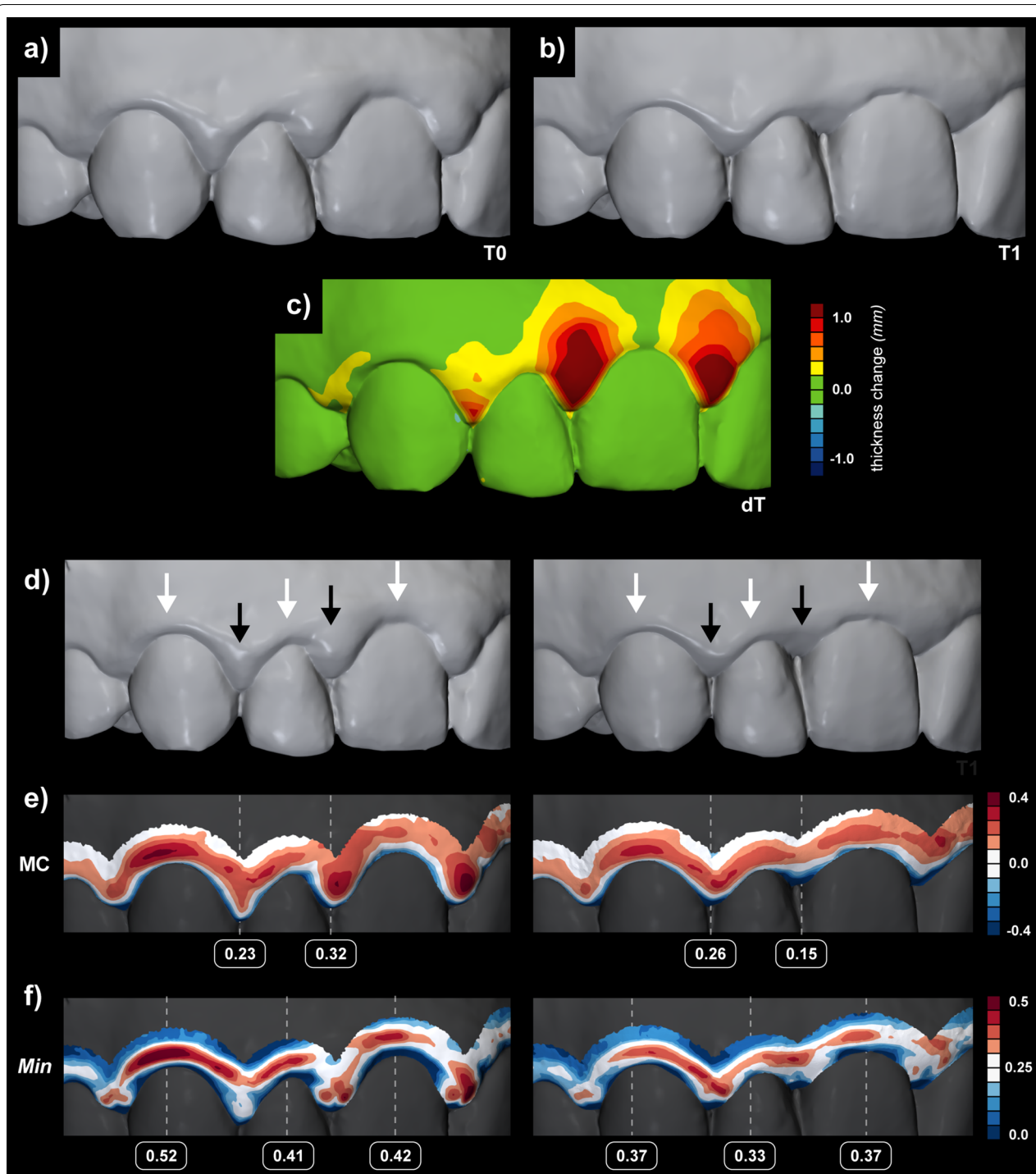


**Fig. 6** Evaluation of soft tissue dynamics associated with periodontitis treatment by volumetric assessment (**a**—baseline scan (T0), **b**—follow-up scan (T1), and **c**—colour-coded map) and a novel gingival shape analysis using surface curvature (**d**—T0 and T1 scans, **e**—mean curvature (MC) and **f**—minimum curvature (Min)). Five different regions were selected based on the colour-coded map (**c**), i.e., two interdental with loss of the tissues above 1.0 mm (black arrows) and three central with changes below the 0.4 mm threshold (white arrows) (**d**)

curvature measures. The shape of the central gingiva mainly depends on the tooth's position in the dental arch, the position of the root in relation to the alveolar process, and the anatomy of the root [48]. Those relations are typically displayed as a mesial-distal convexity of central gingival as observed with a mesial-distal cross-section of a maxillary canine (Fig. 1b) and colour-coded curvature maps using Max (Additional file 1: Fig. 1). In the absence of pathology, the central gingiva is tightly adapted to the underlying hard tissues with a knife-edge margin, i.e., observing the coronal-apical profile [48]. With gingival inflammation, swelling occurs, additionally and reliably displayed with Min (Fig. 5a). In contrast, the shape of the interdental gingiva is more complex. It depends on the contour of the proximal tooth surfaces, underlying bone support, and gingival embrasures' size, shape, and location [48]. As the bone support of two neighbouring teeth may differ, interdental ROI was not further divided into mesial and distal ROI. Observing cross-sections at the interdental gingiva revealed that principal curvatures are contrarywise as with central gingiva and are more similar regarding values (Fig. 1b and c). Therefore, combining both principal curvatures, such as MC, seems better to describe the swollen interdental gingiva (Fig. 5b). However, the analysis with its parameters and clinical relevance needs to be further tested for specific clinical scenarios and datasets to enable practical quantitative gingival shape analysis using optical scans.

For effective implementation of a novel method, comprehensive yet straightforward evaluation and visualisation of all available data is essential. Cross-section image evaluation, which is most extensively used in periodontology and implantology, represents only one of the numerous possible sections that are not being evaluated and displayed. More specifically, the curvature is measured only in the direction of the cross-section (Fig. 1) [46]. In comparison, the 3D approach for evaluating and visualising shape with surface curvature has a significant advantage because it allows measurement of the curvature independent of the specific locations and orientations of imaging. Furthermore, surface curvature analysis is an excellent example of overcoming evaluation with several standardised yet arbitrary preselected measuring sites, potentially omitting relevant information [49]. Such a comprehensive approach may also represent a considerable step toward personalized or precision dentistry [50, 51].

The benefit of intraoral scanning as a diagnostic tool may present an added value to the clinical workflow either in terms of evaluation of disease presence or progression [52, 53]. Despite significant investment in money, intraoral scanners are increasingly present and used in dental practices [54]. Digital models obtained with optical scanning can be magnified and viewed from different

directions, facilitating detailed inspection of the models due to the high resolution [55]. Utilization of intraoral scanning for objective evaluation possibilities, such as follow-up with superimposition of the scans and shape analysis, would enhance a conventional clinical examination and increase early detection. The importance of early detection and prevention of gingivitis as a first step toward preventing periodontitis [56, 57] was also recently emphasized by a recent report on periodontitis' financial and human costs commissioned by the [58].

The present study was subjected to some limitations. First, the proposed method requires specific computer knowledge with 3D analysis software experience. Therefore, open-source software for processing and editing 3D digital models, i.e., MeshLab, was utilised as the leading intuitive and easy software. Furthermore, due to the combination of different settings, many required computations were efficiently performed using basic programming to batch the process. Second, other intraoral scanners should be tested as well. However, regarding surface curvature estimation, the effect of the initial scan, i.e., surface mesh composition, is minimised due to selecting the diameter of interest. Third, selecting a discrete colour scale requires a definition of arbitrarily defined thresholds that may not be yet settled from the perspective of clinical relevance. Further studies are required correlating existing knowledge to define such thresholds.

## Conclusions

Within the limitations of the present study, surface curvature estimation of the intraoral scans seems to be a precise and reproducible method for gingival shape analysis. However, further studies are required to correlate shape in terms of morphological variability and presence of inflammation with clinical data.

## Abbreviations

CSV: Comma-separated values; CU: Curvedness; GC: Gaussian curvature; GS: Gingival shape parameter;  $k_{max}$ : Maximum principal curvature;  $k_{min}$ : Minimum principal curvature; Max: Maximum curvature measure; MC: Mean curvature; Min: Minimum curvature measure; PLY: Polygon file format; ROI: Region of interest; SI: Shape index; STL: Standard Tessellation Language.

## Supplementary Information

The online version contains supplementary material available at <https://doi.org/10.1186/s12903-022-02322-y>.

**Additional file 1: Supplementary Figure 1.** Baseline (T0) and three-month follow-up (T1) after non-surgical periodontal treatment intraoral scans (upper row) were evaluated with gingival shape analysis using surface curvature using available curvature measures. Five different regions were selected to outline the gingival shape changes, i.e., two interdental with loss of the tissues above 1.0 mm (black arrows) and three central with changes below the 0.4 mm threshold (white arrows).

**Acknowledgements**

Not applicable.

**Author contributions**

MKu contributed to conceptualization, methodology, software, validation, formal analysis, investigation, resources, data curation, writing—original draft and review & editing, visualization, and project administration. ACK contributed to validation, investigation, resources, data curation, writing—review & editing, and project administration. RG contributed to investigation, resources, data curation, writing—review & editing, supervision, and project administration. JG contributed to methodology, software, formal analysis, resources, writing—review & editing, and funding acquisition. MKn contributed to methodology, software, formal analysis, resources, writing—review & editing, and funding acquisition. AF contributed to conceptualization, methodology, software, validation, formal analysis, resources, writing—review & editing, visualization, supervision, project administration, and funding acquisition. All authors have read and approved the manuscript.

**Funding**

The work was supported by the Ministry of Higher Education, Science, and Technology, the Republic of Slovenia, under Grant Number P3-0293, P1-0288, J1-3005, N1-0137 and P1-0294. The funding body did not involve in the study design, data collection, data analysis, interpretation of data and writing the manuscript.

**Availability of data and materials**

The data that support the findings of this study are available on a reasonable request from the corresponding author. The data are not publicly available due to privacy or ethical restrictions.

**Declarations****Ethics approval and consent to participate**

The National Medical Ethics Committee of the Republic of Slovenia approved the study (Protocol No. 0120–595/2018/4), and the study was conducted in accordance with the Helsinki Declaration as revised in 2013. All participants gave written informed consent.

**Consent for publication**

Not applicable.

**Competing interests**

The authors declare that they have no competing interests.

**Author details**

<sup>1</sup>Department of Restorative Dentistry and Endodontics, University Medical Centre Ljubljana, Hrvatski trg 6, 1000 Ljubljana, Slovenia. <sup>2</sup>Faculty of Medicine, University of Ljubljana, Ljubljana, Slovenia. <sup>3</sup>Public Health Centre Celje, Celje, Slovenia. <sup>4</sup>Department of Oral Medicine and Periodontology, University Medical Centre Ljubljana, Ljubljana, Slovenia. <sup>5</sup>Department of Oral Medicine and Periodontology, Faculty of Medicine, University of Ljubljana, Ljubljana, Slovenia. <sup>6</sup>Faculty of Mathematics and Physics, University of Ljubljana, Ljubljana, Slovenia. <sup>7</sup>Department of Endodontics and Operative Dentistry, Faculty of Medicine, University of Ljubljana, Ljubljana, Slovenia.

Received: 3 May 2022 Accepted: 5 July 2022

Published: 12 July 2022

**References**

- Preshaw PM. Detection and diagnosis of periodontal conditions amenable to prevention. *BMC Oral Health*. 2015. <https://doi.org/10.1186/1472-6831-15-S1-S5>.
- Lang NP, Bartold PM. Periodontal health. *J Clin Periodontol*. 2018;45:59–16.
- Murakami S, Mealey BL, Mariotti A, Chapple ILC. Dental plaque-induced gingival conditions. *J Clin Periodontol*. 2018;45(February):S17–27.
- Trombelli L, Farina R, Silva CO, Tatakis DN. Plaque-induced gingivitis: case definition and diagnostic considerations. *J Clin Periodontol*. 2018;45:S44–67.
- Malpartida-Carrillo V, Tinedo-Lopez PL, Guerrero ME, Amaya-Pajares SP, Özcan M, Rösing CK. Periodontal phenotype: a review of historical and current classifications evaluating different methods and characteristics. *J Esthetic Restor Dent*. 2021;33:432–45.
- Perillo L, Isola G, Esercizio D, Iovane M, Triolo G, Matarese G. Differences in craniofacial characteristics in Southern Italian children from Naples: a retrospective study by cephalometric analysis. *Eur J Paediatr Dent*. 2013;14:195–8.
- Matarese G, Isola G, Ramaglia L, Dalessandri D, Lucchese A, Alibrandi A, et al. Il biotipo parodontale: Caratteristiche, prevalenze e dimensioni correlati alla malocclusione dentale. *Minerva Stomatol*. 2016;65:231–8.
- Tavelli L, Barootchi S, Majzoub J, Chan HL, Giannobile W, Wang HL, et al. Ultrasonographic tissue perfusion analysis at implant and palatal donor sites following soft tissue augmentation: a clinical pilot study. *J Clin Periodontol*. 2021;48:602–14.
- Probst M, Burian E, Robl T, Weidlich D, Karampinos D, Brunner T, et al. Magnetic resonance imaging as a diagnostic tool for periodontal disease: a prospective study with correlation to standard clinical findings—is there added value? *J Clin Periodontol*. 2021;48:929–48.
- Chung HM, Park JY, Ko KA, Kim CS, Choi SH, Lee JS. Periodontal probing on digital images compared to clinical measurements in periodontitis patients. *Sci Rep*. 2022;12:1–7.
- Walter C, Schmidt JC, Rinne CA, Mendes S, Dula K, Sculean A. Cone beam computed tomography (CBCT) for diagnosis and treatment planning in periodontology: systematic review update. *Clin Oral Investig*. 2020;24:2943–58.
- Kakizaki S, Aoki A, Tsubokawa M, Lin T, Mizutani K, Koshy G, et al. Observation and determination of periodontal tissue profile using optical coherence tomography. *J Periodontol Res*. 2018;53:188–99.
- Rosin M, Splieth C, Hessler M, Gärtner C, Kordaß B, Kocher T. Quantification of gingival edema using a new 3-D laser scanning method. *J Clin Periodontol*. 2002;29:240–6.
- Daly S, Seong J, Parkinson C, Newcombe R, Claydon N, West N. A proof of concept study to confirm the suitability of an intra oral scanner to record oral images for the non-invasive assessment of gingival inflammation. *J Dent*. 2021;105:103579.
- Steinmeier S, Wiedemeier D, Hämmerle CHF, Mühlemann S. Accuracy of remote diagnoses using intraoral scans captured in approximate true color: a pilot and validation study in teledentistry. *BMC Oral Health*. 2020;20:1–8.
- Revilla-León M, Gómez-Polo M, Barmak AB, Inam W, Kan JYK, Kois JC, et al. Artificial intelligence models for diagnosing gingivitis and periodontal disease: a systematic review. *J Prosthetic Dent*. 2022;2022:1–9.
- Galarraga-Vinueza ME, Obreja K, Magini R, Sculean A, Sader R, Schwarz F. Volumetric assessment of tissue changes following combined surgical therapy of peri-implantitis: a pilot study. *J Clin Periodontol*. 2020;47:1159–68.
- Rebele SF, Zuhr O, Schneider D, Jung RE, Hürzeler MB. Tunnel technique with connective tissue graft versus coronally advanced flap with enamel matrix derivative for root coverage: a RCT using 3D digital measuring methods. Part II. Volumetric studies on healing dynamics and gingival dimensions. *J Clin Periodontol*. 2014;41:593–603.
- Schneider D, Grunder U, Ender A, Hämmerle CHF, Jung RE. Volume gain and stability of peri-implant tissue following bone and soft tissue augmentation: 1-year results from a prospective cohort study. *Clin Oral Implants Res*. 2011;22:28–37.
- Kuralt M, Kučić AC, Gašperšič R, Fidler A. Evaluation of gingival recessions with conventional versus digital methods. *J Dent*. 2022;120:104093.
- Schneider D, Ender A, Truninger T, Leutert C, Sahrman P, Roos M, et al. Comparison between clinical and digital soft tissue measurements. *J Esthetic Restor Dent*. 2014;26:191–9.
- Zuhr O, Rebele SF, Schneider D, Jung RE, Hürzeler MB. Tunnel technique with connective tissue graft versus coronally advanced flap with enamel matrix derivative for root coverage: a RCT using 3D digital measuring methods. Part I. Clinical and patient-centred outcomes. *J Clin Periodontol*. 2014;41:582–92.
- Fageeh HN, Meshni AA, Jamal HA, Preethanath RS, Helboub E. The accuracy and reliability of digital measurements of gingival recession versus conventional methods. *BMC Oral Health*. 2019;19:1–8.

24. Griffiths GW, Plociniczak, Schiesser WE. Analysis of cornea curvature using radial basis functions—Part I: methodology. *Comput Biol Med.* 2016;77:274–84.
25. Liu X, Beheshti I, Zheng W, Li Y, Li S, Zhao Z, et al. Brain age estimation using multi-feature-based networks. *Computers in Biology and Medicine.* 2022;143:105285.
26. Bruse JL, McLeod K, Biglino G, Ntsinjana HN, Capelli C, Hsia TY, et al. A statistical shape modelling framework to extract 3D shape biomarkers from medical imaging data: assessing arch morphology of repaired coarctation of the aorta. *BMC Medical Imaging.* 2016;16:1–19.
27. Simon B, Lipták L, Lipták K, Tárnski ÁD, Tárnski DL, Melicher D, et al. Application of intraoral scanner to identify monozygotic twins. *BMC Oral Health.* 2020;20:268.
28. Deferm JT, Schreurs R, Baan F, Bruggink R, Merx MAW, Xi T, et al. Validation of 3D documentation of palatal soft tissue shape, color, and irregularity with intraoral scanning. *Clinical Oral Investigations.* 2018;22:1303–9.
29. Caton JG, Armitage G, Berglund T, Chapple ILC, Jepsen S, Kornman K, et al. A new classification scheme for periodontal and peri-implant diseases and conditions—Introduction and key changes from the 1999 classification. *Journal of Clinical Periodontology.* 2018;45 March:51–8.
30. O'Neill B. Shape operators. In: O'Neill B, editor. *Elementary differential geometry*. 2nd ed. Academic Press: London; 2006. p. 202–62.
31. Koenderink JJ, van Doorn AJ. Surface shape and curvature scales. *Image Vis Comput.* 1992;10:557–64.
32. Guennebaud G, Gross M. Algebraic point set surfaces. *ACM Trans Graph.* 2007;26:23.
33. Meyer M, Desbrun M, Schröder P, Barr AH. *Discrete Differential-Geometry Operators for Triangulated 2-Manifolds*. In: Hege H-C, Polthier K, editors. *Visualization and Mathematics III*. Berlin, Heidelberg: Springer Berlin Heidelberg; 2003. p. 35–57.
34. Fedorov A, Beichel R, Kalpathy-Cramer J, Finet J, Fillion-Robin JC, Pujol S, et al. 3D Slicer as an image computing platform for the Quantitative Imaging Network. *Magn Resonance Imaging.* 2012;30:1323–41.
35. Kuralt M, Fidler A. A novel computer-aided method for direct measurements and visualization of gingival margin changes. *J Clin Periodontol.* 2022;49:153–63.
36. Kuralt M, Gašperšič R, Fidler A. 3D computer-aided treatment planning in periodontology: a novel approach for evaluation and visualization of soft tissue thickness. *J Esthetic Restor Dent.* 2020;32:457–62.
37. Mayer Y, Ginesin O, Machtei EE. Photometric CIELAB analysis of the gingiva: a novel approach to assess response to periodontal therapy. *J Periodontol.* 2017;88:854–9.
38. Smith RN, Lath DL, Rawlinson A, Karmo M, Brook AH. Gingival inflammation assessment by image analysis: measurement and validation. *Int J Dent Hyg.* 2008;6:137–42.
39. Newby EE, Bordas A, Kleber C, Milleman J, Milleman K, Keogh R, et al. Quantification of gingival contour and volume from digital impressions as a novel method for assessing gingival health. *Int Dent J.* 2011;61(Suppl 3):4–12.
40. Thomason JM, Ellis JS, Jovanovski V, Corson M, Lynch E, Seymour RA. Analysis of changes in gingival contour from three-dimensional co-ordinate data in subjects with drug-induced gingival overgrowth. *J Clin Periodontol.* 2005;32:1069–75.
41. Blumer C, Caiani EG, Carminati MC, Cates J, Cattin PC, Cong S, et al. *Statistical shape and deformation analysis: methods, implementation and applications*. 1st ed. London: Elsevier Ltd; 2017.
42. Kuralt M, Gašperšič R, Fidler A. Methods and parameters for digital evaluation of gingival recession: a critical review. *J Dent.* 2021;118:103793.
43. Woodsend B, Koufoudaki E, Mossey PA, Lin P. Automatic recognition of landmarks on digital dental models. *Comput Biol Med.* 2021;137:104819.
44. di Angelo L, di Stefano P, Bernardi S, Continenza MA. A new computational method for automatic dental measurement: the case of maxillary central incisor. *Comput Biol Med.* 2016;70:202–9.
45. Li X, Wang X, Chen M. Accurate extraction of outermost biological characteristic curves in tooth preparations with fuzzy regions. *Comput Biol Med.* 2018;103:208–19.
46. Kuralt M, Gašperšič R, Fidler A. The precision of gingival recession measurements is increased by an automated curvature analysis method. *BMC Oral Health.* 2021;21:1–10.
47. Pottmann H, Wallner J, Huang QX, Yang YL. Integral invariants for robust geometry processing. *Comput Aided Geom Des.* 2009;26:37–60.
48. Bosshardt DD, Lindhe J, Lang NP, Araújo M. Anatomy and histology of periodontal tissues. In: Lang NP, Berglund T, Giannobile W, Sanz M, editors. *Lindhe's clinical periodontology and implant dentistry*. 7th ed. New York: Wiley; 2021.
49. Fidler A, Plotino G, Kuralt M. A critical review of methods for quantitative evaluation of root canal transportation. *J Endod.* 2021;47:721–31.
50. Schwendicke F, Krois J. Precision dentistry—what it is, where it fails (yet), and how to get there. *Clin Oral Investig.* 2022;26:3395–403.
51. Joda T, Yeung AWK, Hung K, Zitzmann NU, Bornstein MM. Disruptive innovation in dentistry: what it is and what could be next. *J Dent Res.* 2020. <https://doi.org/10.1177/0022034520978774>.
52. Michou S, Vannahme C, Ekstrand KR, Benetti AR. Detecting early erosive tooth wear using an intraoral scanner system. *J Dent.* 2020;100:103445.
53. Michou S, Lambach MS, Ntovas P, Benetti AR, Bakhshandeh A, Rahiotis C, et al. Automated caries detection in vivo using a 3D intraoral scanner. *Sci Rep.* 2021;11:21276.
54. Revilla-Leon M, Frazier K, da Costa JB, Kumar P, Duong ML, Khajotia S, et al. Intraoral scanners: An American Dental Association Clinical Evaluators Panel survey. *J Am Dent Assoc.* 2021;152:669–670.e2.
55. Mangano FG, Admakin O, Bonacina M, Lerner R, Rutkunas V, Mangano C. Trueness of 12 intraoral scanners in the full-arch implant impression: a comparative in vitro study. *BMC Oral Health.* 2020;20:1–21.
56. Chapple ILC, van der Weijden F, Doerfer C, Herrera D, Shapira L, Polak D, et al. Primary prevention of periodontitis: managing gingivitis. *J Clin Periodontol.* 2015;42:S71–6.
57. Mariotti A, Hefti AF. Defining periodontal health. *BMC Oral Health.* 2015;15:1–18.
58. European Federation of Periodontology. Time to take gum disease seriously. 2021. [https://www.efp.org/fileadmin/uploads/efp/Documents/Other\\_publications/FINAL\\_article\\_EIU178\\_-\\_Gum\\_Disease\\_-\\_DV5.pdf](https://www.efp.org/fileadmin/uploads/efp/Documents/Other_publications/FINAL_article_EIU178_-_Gum_Disease_-_DV5.pdf).

## Publisher's Note

Springer Nature remains neutral with regard to jurisdictional claims in published maps and institutional affiliations.

**Ready to submit your research? Choose BMC and benefit from:**

- fast, convenient online submission
- thorough peer review by experienced researchers in your field
- rapid publication on acceptance
- support for research data, including large and complex data types
- gold Open Access which fosters wider collaboration and increased citations
- maximum visibility for your research: over 100M website views per year

**At BMC, research is always in progress.**

Learn more [biomedcentral.com/submissions](https://biomedcentral.com/submissions)

